Active Generation and Propagation of Quantum Analogous Spin State of Guided Waves for Topological NDE/SHM

SOURAV BANERJEE, EBRAHIM KHALIL BHUIYAN, ALBERTO DIAZ and SHREE GHOSH

ABSTRACT

The spin topology of guided waves presents new opportunities for Structural Health Monitoring (SHM) and Nondestructive Evaluation (NDE). By leveraging spin-momentum locking, damage detection techniques can be enhanced through controlled wave propagation, enabling selective energy transport and improved sensitivity to structural anomalies. Traditional ultrasonic methods rely on wave reflections and mode conversions, whereas spin-mediated guided waves offer additional degrees of freedom to analyze wave interactions with defects. In this study, the intrinsic quantum analogous spin states of guided ultrasonic waves in elastic waveguides are examined from a quantum-inspired perspective. Unlike conventional interpretations of guided wave propagation, we demonstrate that spin angular momentum (SAM) emerges naturally from the superposition of elastic wave potentials. To apply these principles in SHM and NDE, we propose approaches utilizing conventional piezoelectric transducers and laser-based sensing techniques. In this study the utilization of spin state and its effect on topological geometric phase is demonstrated through virtual experiments. The ability to manipulate spin states in guided waves introduces a promising framework for advanced structural diagnostics, paving the way for more robust and efficient monitoring solutions in engineering applications.

INTRODUCTION

Ultrasonic surface-mounted sensors are widely utilized in Structural Health Monitoring (SHM) due to their ability to generate guided waves capable of probing structural integrity. Piezoelectric wafer sensors, in particular, are effective in exciting, guided wave modes that interact with structural features and defects. These wave modes carry distinct signatures useful for detecting damage [1, 2].

Sourav Banerjee, Mechanical Engineering, University of South Carolina, 300 Main Street, Columbia, South Carolina, 29063, U.S.A.
Ebrahim Khalil Bhuiyan, Mechanical Engineering, University of South Carolina, 300 Main Street, Columbia, South Carolina, 29063, U.S.A.

Damage may be inferred from amplitude reduction when waves encounter defects along the propagation path or from reflection, scattering, and mode conversion when defects are located off-axis. However, in isotropic or symmetric media, defect localization remains ambiguous—especially for so-called "mirrored damages" symmetrically located on either side of the wave path. Without geometric triangulation, traditional ultrasonic NDE struggles with directional specificity.

Another limitation is the influence of environmental factors, particularly temperature, which alter material properties and, consequently, wave characteristics. Finding wave features that remain invariant under environmental conditions would significantly advance NDE and SHM capabilities. In this context, the present study explores spin-quantized ultrasonic guided waves, leveraging topological geometric phases derived from quantum analogues [3, 4]. These spin-dependent features offer potential for detecting mirrored damages and improving localization.

Elastic guided waves consist of both longitudinal (P) and shear (S) wave components, whose superposition results in symmetric and antisymmetric modes within bounded media. Recent research has highlighted quantum-analogous phenomena in guided waves, including spin-orbit interactions (SOI) and spin-momentum locking [4, 5], which may co-exist in a structure during the wave propagation. Spin states confined to the thickness direction spatially distributed spin states that could be more sensitive to defect positioning could be induced by SOI.

Spin-redirection and SOI are shown to generate topological geometric phases over non-periodic structures by rotating the displacement field in real space, not just reciprocal space [6, 7]. This is akin to the Möbius-like transformation of spin vectors observed in acoustic vortex beams and helical wave transport [8–10]. The link between spin state evolution and geometric phase [11–14], as well as phenomena such as spin-momentum locking and the quantum spin Hall effect (QSHE) in acoustics and elasticity [3, 15], underscore the physical basis for this approach. Although prior studies have attempted to quantify topological phases from guided wave data in limited Fourier space [16], spin state fundamentals were often overlooked. This work addresses that gap by analyzing the origin and implications of spin states in ultrasonic guided waves for improved SHM and NDE.

MATERIALS AND METHODS

The use of the conserved Noether current provides a powerful framework to investigate spin state energy propagation and its contribution to total angular momentum in elastic waveguides. Based on Noether's theorem, which links symmetries of physical systems to conservation laws, the method starts with the Hamilton principle and Euler-Lagrange formalism to derive the governing equations for a displacement wave field in an elastic medium. The Lagrangian density is formulated as the difference between kinetic and strain energy densities, leading to the energy-momentum tensor. Through spacetime transformations and infinitesimal variations in displacement, the conserved energy-momentum tensor is expressed, setting the stage for analyzing wave-induced angular momentum.

Further, by introducing rotational coordinate transformations, the spin and orbital contributions to angular momentum in the waveguide are separated, paralleling the quantum mechanical distinction between spin angular momentum (SAM) and orbital angular momentum (OAM). The Noether current, derived from the rotated displacement field, contains two components: an origin-dependent part associated with OAM and an origin-independent component linked to SAM. The SAM density is shown to depend solely on the cross product of the displacement and its time derivative, emphasizing its independence from material properties and spatial coordinates. This framework thus enables a complete and physically consistent understanding of angular momentum propagation in elastic waveguides, analogous to quantum systems. The Noether current J_k will be equal to the total momentum density

$$J_k = \epsilon_{kjm}\ x_j T_{m0} + \epsilon_{kmj}\ u_m \frac{\partial \mathcal{L}}{\partial(\dot{u}_j)}. \tag{1}$$

In quantum mechanics for $\alpha = 0$ total angular momentum is always divided into two parts, OAM and SAM, in elastic solid it could also be written as follows.

$$J_k = L_k + S_k \tag{2}$$

Where, due to the inherent space term the L_k describes the origin dependent Noether current, which is OAM density, whereas S_k is independent of material properties and independent of choice of origin. S_k can be expressed as

$$S_k = \epsilon_{kmj}\ \rho u_m \dot{u}_j \qquad \text{or} \quad \boldsymbol{S} = \rho \left[\!\left[\ [\mathbf{u}] \times \left[\frac{d\mathbf{u}}{dt}\right] \right]\!\right]_t \tag{3}$$

The elastic SAM density in Eq. (3) is only dependent on the simultaneous change in polarity of the wave filed over time.

Expressing the Spin using Displacement Field

Considering guided wave modes associated with one longitudinal and two transverse wave amplitudes, the spin states resulted from their internal interaction could be mathematically written as

$$s_k(x_n, t) = \epsilon_{kmj}\ \rho u_m \dot{u}_j = \\ -i\rho\omega \left\{ \begin{matrix} \epsilon_{kmj} \cdot \left[\left[ik_m^p A e^{i(k_n^p x_n)}\right] + \left[i\ \hat{\mathbf{e}}_m \epsilon_{mlq} \mathrm{B}_q k_l^s e^{i(k_n^s x_n)}\right]\right]. \\ \left[\left[ik_j^p A e^{i(k_n^p x_n)}\right] + \left[i\ \hat{\mathbf{e}}_j \epsilon_{jlq} \mathrm{B}_q k_l^s e^{i(k_n^s x_n)}\right]\right] \end{matrix} \right\} \tag{4}$$

Where, ρ is the material density and ω is the frequency of wave propagation. At any point x_k in a wave guide, let's assume the three-dimensional displacement field $\mathbf{u}(x_k, t) = \{u_1(x_k, t) \quad u_2(x_k, t) \quad u_3(x_k, t)\}^T$ over time. Knowing the quantum spin matrices, evolution of the SAM density in space and time and its respective vector pointing the spin could be identified as follows.

$$\mathbf{s}(x_j,t) = \frac{\rho\omega}{2}[\mathbf{u}^*\boldsymbol{\sigma}_1\,\mathbf{u} + \mathbf{u}^*\boldsymbol{\sigma}_2\,\mathbf{u} + \mathbf{u}^*\boldsymbol{\sigma}_3\mathbf{u}] = \frac{\rho\omega}{2}\langle\mathbf{u}|\widehat{\boldsymbol{\Sigma}}|\mathbf{u}\rangle \tag{5}$$

Or

$$\mathbf{s}(x_j,t) = \hat{\mathbf{e}}_{\boldsymbol{k}}\frac{\rho\omega}{2}\,u_i{}^*\boldsymbol{\sigma}_k^{ij}u_j \tag{6}$$

In this context, spin is treated as a vector field [16, 17] that evolves over time. It arises from the instantaneous local dynamics of the wave field—such as the circular or elliptical trajectory traced by particle motion at a given location. For acoustic or elastic waves, the spin vector is commonly expressed as the cross product between the displacement and velocity vectors. Since these quantities oscillate, particularly in harmonic fields, the resulting spin varies with time and forms an elliptical path over a single wave period. To analyze steady-state properties like momentum transport, energy flow, or mode structure, it is often more insightful to consider the spin angular momentum (SAM), which is defined as the time-averaged version of the spin vector over a wave cycle. Although SAM and the instantaneous spin vector may appear distinct at first, they represent the same physical concept when interpreted carefully in their respective contexts. In Eq. (5) and (6) the $\boldsymbol{\sigma}_i$ matrices could be written and visualized as it is depicted in Figure **1**.

Topological: Spin and Geometric Phase

Spin angular momentum (SAM) represents the intrinsic angular momentum arising from the polarization of displacement vectors within the wave field. It can be seen that the displacement vectors [17] exhibit circular polarization, which gives rise to a spin angular momentum density described by Eq. (6). The direction of this spin is determined by the sign of $\mathbf{s}(x_j,t)$: a positive value indicates counterclockwise rotation, while a negative value corresponds to clockwise rotation, following the right-hand rule in a Cartesian coordinate system.

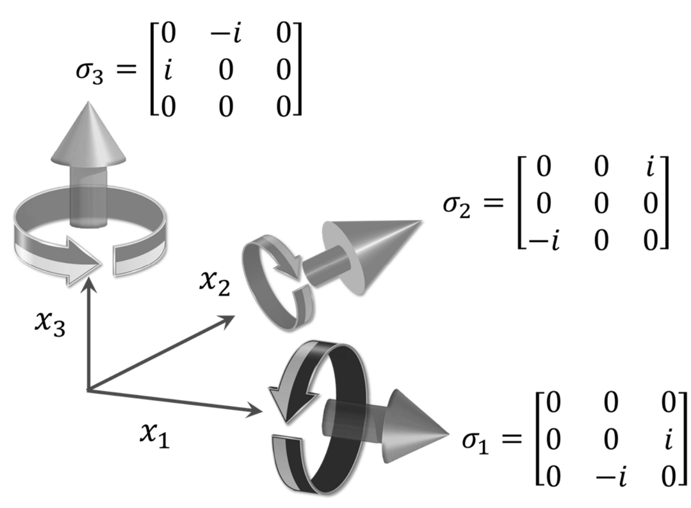

Figure **1**: Spin matrix components. These three components are $\boldsymbol{\sigma}_1$, $\boldsymbol{\sigma}_2$ and $\boldsymbol{\sigma}_3$

Additionally, the geometric phase is defined as the phase shift accumulated by a wave due to the spatial evolution of its polarization or spin state. It is evident from Ref [17] that SAM and geometric phase are inherently connected through the wave's polarization characteristics. This relationship can be quantitatively described when integrated over a specific path, such as the propagation of the wave from the incidence point toward the northeast (NE) or northwest (NW) damage region and its subsequent refraction toward the probe location. Relation between the Geometric phase and SAM density in Eq. (6) could be expressed as

$$\emptyset_g = \int \frac{\mathbf{s}(x_j,t)}{\hbar} d\mathbf{x} \quad \text{and} \quad \mathbf{s}(x_j,t) = \hbar \frac{\partial \emptyset_g}{d\mathbf{x}} \tag{7}$$

for elastic waves normalized $\hbar = 1$ and $\mathbf{x}$ is in cartesian coordinate along the wave path.

Experimental Design

In this virtual experiment, a PZT sensor is positioned at $x_1 = 0\,;\, x_2 = 40\,mm$, relative to the center of a hexagonal PZT cluster. A probe point is placed slightly below at $x_1 = 0\,;\, x_2 = 36\,mm$ mm to record orthogonal displacement components (u_i). To simulate damage, two 3 mm diameter circular holes were introduced—one in the northeast (NE) quadrant at $x_1 = 30\,mm, x_2 = 25\,mm$, and another in the northwest (NW) quadrant at $x_1 = -30\,mm, x_2 = 25\,mm$.

To generate spin-orbit interaction (SOI), each PZT is excited with a 250 kHz 5-cycle tone burst, using phase lags of $-\pi/3$ for anticlockwise spin (ACWS) and $+\pi/3$ for clockwise spin (CWS). Several cases were run across three damage conditions ('No Damage', 'Damage NE', 'Damage NW') and three spin states ('No Spin' with $\varphi = 0$, 'ACWS', and 'CWS'). The time-domain displacement profiles at the probe point for all nine cases were calculated. The results show clear differences in the waveforms depending on the spin state, even when the damage location is unchanged. Particularly, the displacement profiles differ between ACWS and CWS states when damage is located in the NE versus NW quadrant—differences not observed in the No Spin case. These variations are attributed solely to the effects of SOI. Figure **2** illustrates the time evolution of polarity vectors in a three-dimensional representation of these evolving polarity vectors.

To further extract the geometric phase from SAM or polarization orientation, Fig. 2 is analyzed in detail. In the absence of spin-orbit interaction (No SOI, first column), the displacement vectors—green (u_{12}), blue (u_{13}), and magenta (u_{23}) evolve similarly, regardless of whether damage is in the NE or NW quadrant. Further, the temporal evolution of displacement polarity was analyzed through polar plots (not shown).

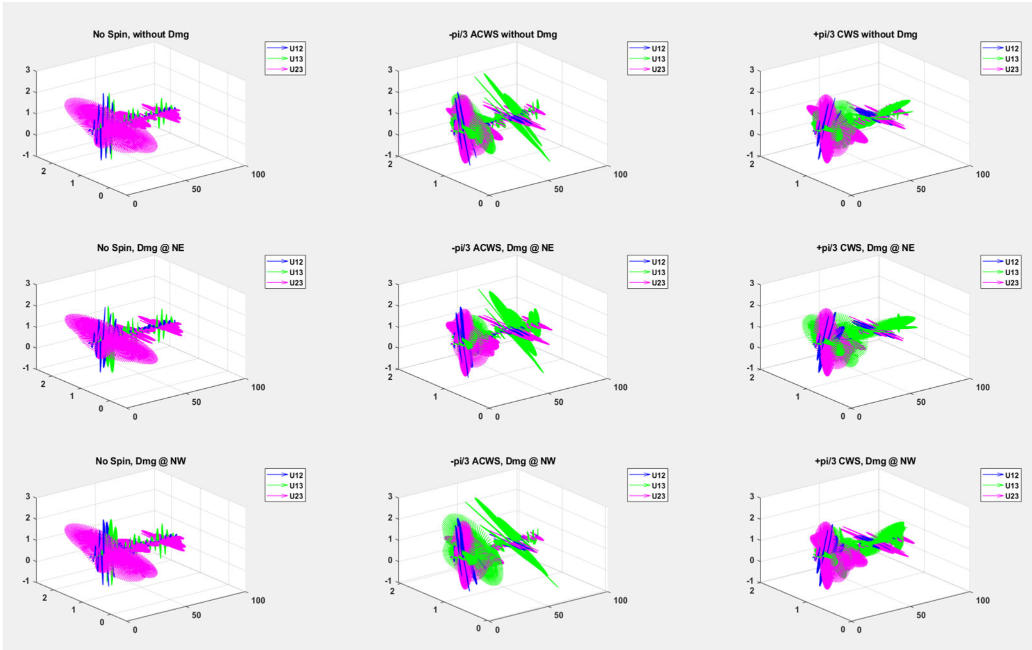

Figure **2**: 3D visualization of displacement field polarization vectors from a virtual NDE/SHM experiment. Blue, green, and magenta vectors represent polarization in the $x_1 - x_2$, $x_1 - x_3$ plane and $x_2 - x_3$ planes, respectively. Rows correspond to damage states: no damage (top), damage in the NE quadrant (middle), and damage in the NW quadrant (bottom). Columns show spin phase conditions: no spin $\varphi = 0$ (left), anticlockwise spin $\varphi = -\pi/3$ (center), and clockwise spin $\varphi = +\pi/3$ (right).

ANALYSIS RESULTS

The temporal evolution of displacement field polarization was analyzed by projecting vectors onto the $x_1 - x_3$ and $x_1 - x_2$ planes, focusing on the behavior of u_{13} (through-thickness) and u_{12} (in-plane) components. Without SOI (i.e., no spin), no significant polarity changes were observed across damage states—indicating topologically equivalent geometric phases. However, with spin activated (ACWS or CWS), distinct polarization patterns emerged. In the pristine state, ACWS and CWS produced mirrored orientations along ~60° and ~20°, respectively. When damage was present, phase accumulations were detected: ACWS resulted in a ~+14.6° shift for NW damage, and CWS led to ~−13.5° for NE damage.

Similarly, for u_{12}, an additional rotational lobe was identified. The main and secondary lobes also showed mirrored behavior under ACWS and CWS (~42° and ~138°, respectively). Phase accumulations of ~+9.8° (ACWS, NW) and ~−10.1° (CWS, NE) were recorded. These consistent shifts across both planes demonstrate that SOI enables clear distinction between NE and NW damage locations, supporting its use in NDE/SHM applications.

CONCLUSION

This study identifies spin-orbit interaction (SOI) as a key mechanism for enhancing the spin angular momentum (SAM) density in guided wave modes. Since guided wave displacement fields are formed by superposing multiple scalar and vector potentials, understanding the interactions among these components is crucial for analyzing spin behavior. Starting from classical and quantum mechanics, a conserved Noether current was derived, leading to an expression for SAM density in terms of complex displacement functions.

A virtual experiment demonstrated that SOI amplifies the sensitivity of polarization vector shifts due to damage. Without SOI, mirrored damage scenarios (e.g., NE vs. NW) are indistinguishable; however, activating ACWS or CWS spin states produces measurable differences in geometric phase. These findings confirm that spin states are quantifiable, and hold promise for advanced NDE and SHM applications.

REFERENCE

1. Auld, B.A., *Acoustic Fields and Waves in Solids*. Vol. I & II. 1973, New York: John Wiley & Sons.
2. Rose, J.L., *Ultrasonic Waves in Solid Media*. 1999, Cambridge: Cambridge University Press.
3. Chengzhi Shi, R.Z., Yang Long, Sui Yang, Yuan Wang, Hong Chen, Jie Ren, Xiang Zhang, *Observation of acoustic spin.* National Science Review, 2019. **6**(4): p. 707-712.
4. Long, Y., J. Ren, and H. Chen, *Intrinsic spin of elastic waves.* Proceedings of the National Academy of Sciences, 2018. **115**(40): p. 9951-9955.
5. Banerjee, S., *Quantum Analogous Spin States of Ultrasonic Guided Waves* Ultrasonics, 2025. **146**: p. 107478.
6. Wang, S., Ma, G., Chan, C. T., *Topological transport of sound mediated by spin-redirection geometric phase.* Science Advances, 2018. **4**(2).
7. Huber, S.D., *Topological mechanics.* Nature Physics, 2016. **12**(7): p. 621-623.
8. Zhang, L., Marston, P. L., , *Angular momentum flux of nonparaxial acoustic vortex beams and torques on axisymmetric objects.* Phys. Rev. E, 2011. **84**(065601(R)): p. 065601-1-5.
9. Zhang, L., Marston, P. L.,, *Acoustic radiation torque on small objects in viscous fluids and connection with viscous dissipation.* J. Acoust. Soc. Am., 2014. **136**: p. 2917-2921.
10. Ma, G., Xiao, M., Chan, C.T, *Topological phases in acoustic and mechanical systems.* Nature Reviews Physics, 2019. **1**: p. 281–294.
11. Zhang, X., et al., *Topological sound.* 2018. **1**(1): p. 1-13.
12. Fleury, R., et al., *Sound isolation and giant linear nonreciprocity in a compact acoustic circulator.* 2014. **343**(6170): p. 516-519.
13. Ni, X., et al., *Topologically protected one-way edge mode in networks of acoustic resonators with circulating air flow.* 2015. **17**(5): p. 053016.
14. Yang, Z., et al., *Topological acoustics.* 2015. **114**(11): p. 114301.
15. Bliokh, K.Y., Nori, F., , *Transverse spin and surface waves in acoustic metamaterials* Physical Review B, 2019. **99**: p. 020301.
16. Zhang, G., Kundu, T., Deymier, P. A., Runge, K., *Defect localization in plate structures using the geometric phase of Lamb waves.* Ultrasonics, 2025. **145**: p. 107492.
17. Banerjee, S., Quantum analogous spin states to explain topological phase for guided waves in ultrasonic nondestructive evaluation, The Journal of the Acoustical Society of America 157 (4), 2477-2497